



OPEN ACCESS

EDITED BY Elisabetta Buommino, University of Naples Federico II, Italy

Luigia Turco Bambino Gesù Children's Hospital (IRCCS). Naglaa Hamdy, Desert Research Center, Egypt

*CORRESPONDENCE Yuanyuan Ma Peng Xue pengxue@ntu.edu.cn Xinyuan Zhao

[†]These authors have contributed equally to this work and share first authorship

RECEIVED 18 September 2025 ACCEPTED 27 October 2025 PUBLISHED 05 November 2025

CITATION

Zheng D, Zhou Y, Xu B, Bu W, Wang F, Zhao X, Xue P and Ma Y (2025) Polystyrene nanoparticles reduce the Cryptococcus neoformans virulence via induction of mitochondrial dysfunction. Front. Cell. Infect. Microbiol. 15:1708192. doi: 10.3389/fcimb.2025.1708192

© 2025 Zheng, Zhou, Xu, Bu, Wang, Zhao, Xue and Ma. This is an open-access article distributed under the terms of the Creative Commons Attribution License (CC BY). The use, distribution or reproduction in other forums is permitted, provided the original author(s) and the copyright owner(s) are credited and that the original publication in this journal is cited, in accordance with accepted academic practice. No use, distribution or reproduction is permitted which does not comply with these terms.

Polystyrene nanoparticles reduce the Cryptococcus neoformans virulence via induction of mitochondrial dysfunction

Dongnan Zheng^{1†}, Yifan Zhou^{1†}, Bin Xu^{2†}, Wenxia Bu¹, Fengxu Wang¹, Xinyuan Zhao^{1*}, Peng Xue^{1*} and Yuanyuan Ma^{1*}

¹Nantong Key Laboratory of Environmental Toxicology, Institute for Applied Research in Public Health, School of Public Health, Nantong University, Nantong, China, ²Jiangxi Key Laboratory of Oncology(2024SSY06041), JXHC Key Laboratory of Tumor Metastasis, Jiangxi Cancer Hospital, The Second Affiliated Hospital of Nanchang Medical College, Nanchang, China

Introduction: Cryptococcus neoformans is a fungus that poses a significant threat to human health, with its polysaccharide capsule being a key virulence factor that can upregulate the expression of host gene ARG1, encoding arginase-1, which suppresses T-cell-mediated antifungal immune responses. Nanoplastics may cause oxidative and mitochondrial stress in mammalian cells, potentially impacting fungal physiology and pathogenic mechanisms as well.

Methods: We utilized mouse models and fungal burden assays to investigate the effects of polystyrene nanoparticles (PS-NPs) on C. neoformans infection. Mice were subjected to oropharyngeal aspiration of 50 µl of 80 nm PS-NPs at a concentration of 5 µg/µl, administered three times a week over a specified duration. To assess the impact of PS-NPs on C. neoformans mitochondria, we measured intracellular reactive oxygen species (ROS) levels, mitochondrial superoxide, mitochondrial membrane potential, and intracellular ATP levels in whole fungal cells. Additionally, we performed RNA-Seq analysis and metabolomics studies to evaluate the effects of PS-NPs at a concentration of 0.3 μg/μL on the RNA and metabolic profiles of *C. neoformans* mitochondria.

Results: Our study demonstrated that PS-NPs significantly prolonged the survival of mice infected with C. neoformans (P = 0.0058). PS-NPs exposure resulted in a 30% reduction in ARG1 mRNA expression and enhanced T-cell-mediated antifungal immunity. Additionally, PS-NPs inhibited fungal capsule formation by approximately 40% in infected mice and 70% in capsule induction medium. Given the close link between the mitochondria of C. neoformans and capsule formation, we further investigated the effects of PS-NPs on mitochondrial function. Exposure to PS-NPs led to mitochondrial dysfunction in C. neoformans, as evidenced by a threefold increase in ROS, a 1.7-fold increase in mitochondrial membrane potential, and disruptions in mitochondrial transcription and metabolism.

Conclusion: These results suggest that PS-NPs inhibit the formation of the *C. neoformans* capsule, potentially by inducing mitochondrial dysfunction. Furthermore, the findings highlight the broader implications of PS-NPs on fungal virulence and the dynamics of host-pathogen interactions, underscoring their significance in advancing our understanding of these complex relationships.

KEYWORDS

Cryptococcus neoformans, polystyrene nanoparticles, virulence, capsule, mitochondrial dysfunction

1 Introduction

Cryptococcus neoformans is a significant pathogen capable of causing cryptococcal meningoencephalitis, particularly in individuals with compromised immune systems, such as those with HIV/AIDS. Annually, the disease results in approximately 223,100 deaths within this population (Park et al., 2009; Rajasingham et al., 2017). The World Health Organization recognizes C. neoformans as one of four critical priority fungal pathogens (Casalini et al., 2024). Upon inhalation, this fungus primarily infects the lungs before disseminating to the brain, with CD4⁺ T cell-mediated immunity playing a crucial role in controlling the infection. However, C. neoformans has a unique ability to suppress immune function, leading to reduced cellmediated immunity and heightened pro-inflammatory responses (Huffnagle et al., 1991). Within the key virulence factor capsule of *C*. neoformans, the polysaccharide glucuronoxylomannan plays a significant role in triggering the recruitment of neutrophilic myeloid-derived suppressor cells in both mice and patients diagnosed with cryptococcosis (Li et al., 2022). The binding of glucuronoxylomannan to the C-type lectin receptor-2d enhances the immunosuppressive activity of these cells. This binding event initiates the activation of the p38 pathway, leading to the production of arginase-1 (ARG1), which further inhibits T-cellmediated antifungal responses (Li et al., 2022).

In recent years, environmental concerns about microplastics and nanoplastics have surged due to their pervasive presence and potential detrimental impacts across various ecosystems (Ding et al., 2021; Barguilla et al., 2022; Liu et al., 2022; Li et al., 2023; Tang et al., 2023; Zhai et al., 2024; Bu et al., 2025; Cheng et al., 2025). Emerging evidence suggests that nanoplastics, including polystyrene nanoparticles (PS-NPs), can interact with biological systems, potentially influencing fungal pathogenicity (Ma et al., 2025b). In this study, we examined the effect of PS-NPs on *C. neoformans* infection and found that PS-NPs enhanced survival of *C. neoformans*-infected mice by inhibiting the fungal capsule formation. This study provides new insights into the various impacts of PS-NPs.

2 Materials and methods

2.1 Strains and media

The H99 strain of *C. neoformans* var. *grubii*, classified as serotype A (MAT α), was cultured and maintained on yeast extract peptone dextrose (YPD) medium, which consists of 2% peptone, 1% yeast extract, and 2% dextrose. Additionally, yeast nitrogen base (YNB) medium and capsule induction medium (lowiron medium) were used, prepared according to the methods described in previous studies (Vartivarian et al., 1993; Jung et al., 2008; Saikia et al., 2014).

2.2 Mouse models and fungal burden assay

Male BALB/c mice (6-7 weeks old) were obtained from the Experimental Animal Center at Nantong University (Nantong, China) for virulence assays. Wild-type (WT) C. neoformans cells were cultured overnight in YPD medium at 30°C under shaking (130 rpm), washed with phosphate buffered saline (PBS), and resuspended at a concentration of 1×10 cells ml⁻¹ in PBS. Inoculation was performed by intranasal instillation of 50 µl of the cell suspension, corresponding to an inoculum of 5×10^2 cells per mouse. The first group of 11 mice infected with the WT strain received 50 µl of 5 µg/µl PS-NPs (80 nm) treatment via oropharyngeal aspiration three times a week (Tuesday, Thursday, and Saturday). The second group of 11 infected mice were treated with PBS. The other two groups, without infection, received only PBS or PS-NPs. Mice were monitored daily for health status, and those reaching the humane endpoint were euthanized using CO2 asphyxiation. After 28 days post-inoculation, infected mice were euthanized using CO₂ inhalation to evaluate fungal loads in organs. Their organs were removed, weighed, and homogenized in 1 ml of PBS with a MixerMill (Retsch). Serial dilutions of the homogenates were plated on YPD agar plates containing 35 µg/ml chloramphenicol, and the number of colony-forming units (CFUs) was determined after 48 hours of incubation at 30°C.

Ethical guidelines regarding animal use set by Nantong University were strictly adhered to, ensuring minimal suffering for all mice.

2.3 Capsule analysis

To analyze the capsule of *C. neoformans* cells in the lungs, lung tissues were fixed in 4% paraformaldehyde, embedded in paraffin, and sectioned into 3 μ m slices. Hematoxylin and eosin (HE) staining was performed, and the sections were examined under Nikon ECLIPSE Ti2 microscopy. For capsule analysis of *C. neoformans* in the capsule induction medium, the cells were cultured in the medium for 18 h with or without PS-NPs (0.3 μ g/ μ l) at 30 °C under shaking at 130 rpm. Subsequently, measurements were taken for cell diameter, and capsule size of cells staining with India ink. A total of 50 cells were analyzed per condition, and the data were quantified using ImageJ software. Statistical analyses were performed to assess differences between groups. Data are presented as mean \pm standard deviation (SD). To determine statistical significance, a t-test (two-tailed) was utilized.

2.4 Measurement of intracellular ROS levels, mitochondrial superoxide and mitochondrial membrane potential and intracellular ATP level

C. neoformans cells were cultured overnight at 30°C with shaking at 130 rpm in YPD medium. The cells were then washed twice with PBS and inoculated at an OD₆₀₀ of 0.8 in capsule induction medium, with or without 80 nm non-fluorescent PS-NPs (0.3 µg/µl), and incubated for 18 hours at 30 °C with shaking at 130 rpm. For the assessment of intracellular ROS and mitochondrial function, cells were subsequently stained for various assays. To detect intracellular ROS, cells were incubated with 2',7'-Dichlorofluorescein Diacetate (DCFH-DA, 16 µM) at 30°C for 1 hour. Mitochondrial superoxide levels were measured by treating the cells with Mito-SOX Red (50 mM) under the same conditions. For assessing mitochondrial membrane potential, cells were stained with Mito-Tracker Red CMXRos (Mito-Tracker, 50 nM) for 1 hour at 30°C. The fluorescence intensity of the stained cells (5×10⁷) was measured using a multimode microplate reader (TECAN Infinite E Plex). Intracellular ATP levels were quantified using the BacTiter-Glo Microbial Cell Viability Assay kit (Promega, USA), with signal detection performed on the same microplate reader (TECAN Infinite E Plex). Fluorescence data were normalized to the total cell number to ensure comparability across samples. The experiment was conducted in triplicate.

2.5 RNA-seq analysis

To investigate the effects of PS-NPs on the transcriptome of *C. neoformans*, WT cells were cultivated in YPD medium at 30°C for 16

hours. After washing, the cells were adjusted to a concentration of 4.0 \times 10⁷ cells/mL in YNB medium, with or without the addition of 80 nm non-fluorescent PS-NPs at 0.3 µg/µL. Following an 18-hour incubation, the cells were harvested, washed, and flash-frozen in liquid nitrogen. Total RNA was extracted from the cell pellets using TRIzol. RNA concentration and integrity were assessed using standard methods. Indexed RNA-Seq libraries were generated from 800 ng of total RNA and sequenced on an Illumina HiSeq2500 platform. Read alignment was conducted using Bowtie, and transcript abundances were determined via the RNA-Seq by expectation-maximization tool. Differentially expressed genes (DEGs) were identified with a false discovery rate (FDR) < 0.05 and fold change (FC) ≥ 2. Expression data visualization, including volcano plots, was performed using R (version 4.2.2) and the ggplot2 package. Gene Ontology (GO) analysis was conducted for DEGs using the GO database (Ashburner et al., 2000), and significantly enriched terms were identified using a hypergeometric test. KEGG pathway analysis was used for functional annotation (Kanehisa and Goto, 2000). Validation of RNA-Seq results was performed with quantitative PCR (qPCR) using specific primers (see Supplementary Table S1 for details).

2.6 Metabolomics studies

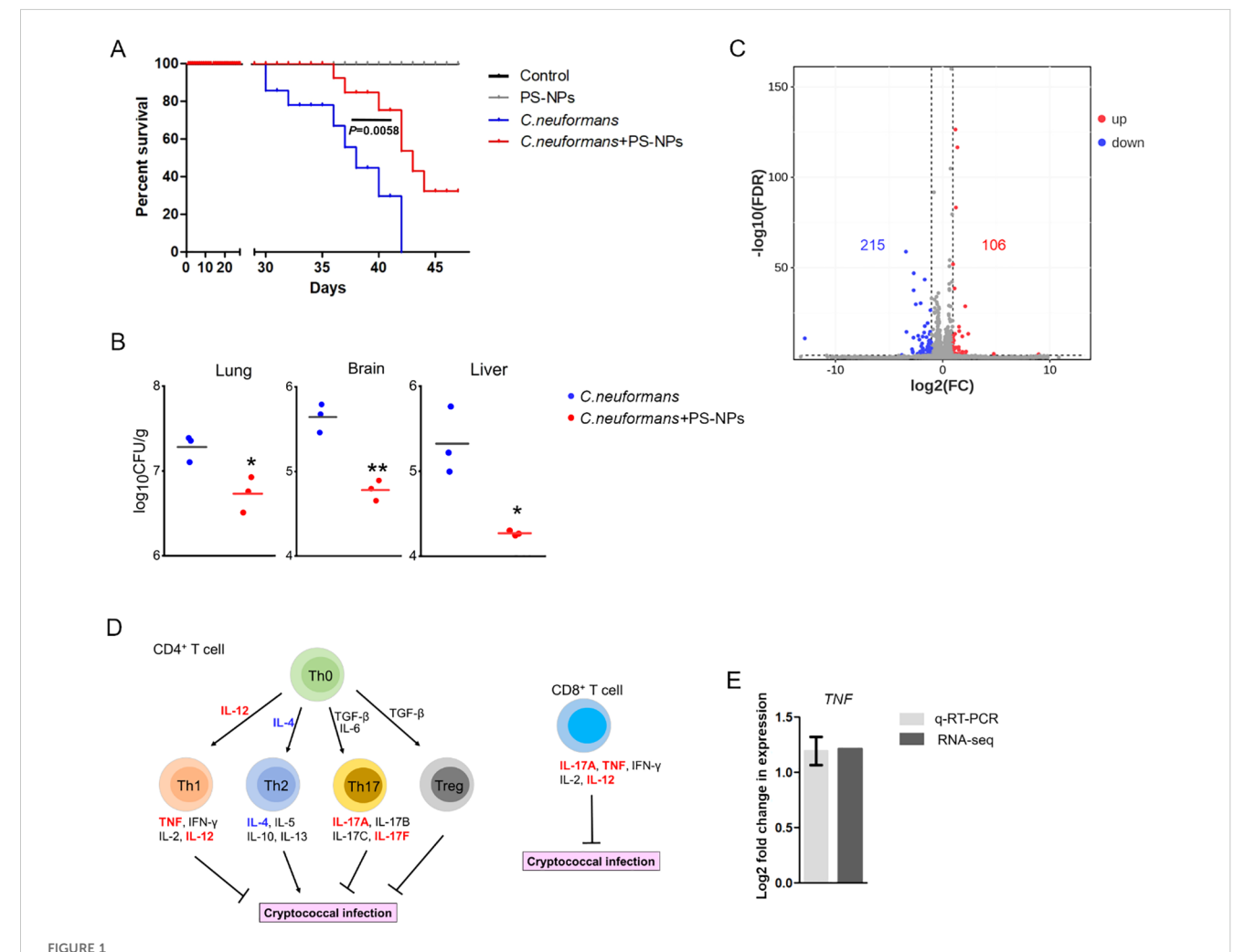
To evaluate the impact of PS-NPs on metabolomics, we cultured three replicate cultures of C. neoformans WT cells in YPD medium for 16 hours at 30 °C. After washing, cells were adjusted to a specific concentration in YNB medium, either with or without PS-NPs, and incubated for an additional 18 hours at 30°C. Following harvest and washing, the cells were frozen in liquid nitrogen. The freeze-dried pellets (~80 mg) were pulverized, and 1000 µL of a methanol/acetonitrile/water (2:2:1, v/v/v) solution was added for metabolite extraction. After centrifugation at 14,000 g and 4 °C for 15 minutes, the supernatant was evaporated, and the samples were reconstituted in 100 µL of acetonitrile/water (1:1, v/v) for LC-MS analysis. We used a UHPLC system coupled with a quadrupole time-of-flight mass spectrometer to perform HILIC separation. The mobile phase consisted of ammonium acetate and ammonium hydroxide in water, and acetonitrile, with a gradient profile tailored for optimal metabolite resolution. Mass spectrometry parameters were set for both positive and negative ion modes, scanning m/z ranges of 60-1000 Da and 25-1000 Da, respectively. Quality control (QC) samples were included to monitor systematic errors during extraction and analysis (Dunn et al., 2011). Metabolite data were normalized based on total peak area to ensure consistency across samples. Principal Component Analysis (PCA) was performed using the gmodels package in R (Warnes et al., 2015), and metabolites with a p-value of <0.05 from differential analysis were identified. The KEGG database was utilized for pathway enrichment analysis, with FDR correction (threshold set at FDR ≤ 0.05) applied to determine significantly enriched pathways associated with the differential metabolites (Kanehisa and Goto, 2000).

3 Results

3.1 PS-NPs exposure mitigates *C. neoformans* infection

Exposure to 80 nm diameter PS-NPs significantly prolonged the survival of mice infected with the *C. neoformans* strain H99, with a survival analysis indicating a statistically significant improvement (P = 0.0058) (Figure 1A). Furthermore, treatment with PS-NPs led to a notable reduction in fungal burden in the lung, brain, and liver

tissues of infected mice, with statistical analysis showing P < 0.05 across these organs (Figure 1B). These findings imply that PS-NPs can effectively mitigate C. neoformans infection. To understand the underlying immune mechanisms, we explored the influence of PS-NPs on T cell-mediated immune responses against C. neoformans. RNA-Seq analysis comparing the transcript profiles of mouse lung tissue from PS-NPs-exposed and non-exposed mice revealed changes in the expression of 321 genes, with 106 genes being upregulated and 215 downregulated (Figure 1C). We focused on the transcript levels of T-cell cytokines known to play critical roles in the host defense



PS-NPs attenuate *C. neoformans* virulence in the mice model of inhalation exposure. **(A)** Survival curve. Male BALB/c mice were intranasally infected with 5×10^2 cells of the WT strain (H99), then divided into two groups after one day. One group received $50 \mu l$ of $0.08 \mu m$ PS-NPs at a concentration of $5 \mu g/\mu l$ three times a week; the other group received PBS. Survival differences were analyzed using the log rank Mantel-Cox test. **(B)** Fungal burden. Fungal cells in the lungs, brains, and livers of infected mice were assessed after 28 days. Significant differences were observed between the two treatment groups as determined by the Mann-Whitney U test (*, P<0.05; **, P<0.01). **(C)** Gene regulation. Analysis revealed 215 downregulated (green) and 106 upregulated (red) genes in the lungs of infected mice treated with or without PS-NPs after 28 days. **(D)** Cytokine expression. PS-NPs regulated T-cell cytokine gene expression, highlighted by upregulated genes in red and downregulated genes in blue. **(E)** TNF gene expression. Transcript levels of the TNF gene were compared via RNA-Seq and qRT-PCR, with a significance threshold of P<0.05 and fold change cut-off ≥ 2 .

against cryptococcal infections. Notably, transcripts for cytokines TNF, IL-12, IL12A, and IL17F were upregulated in response to PS-NPs exposure, indicating a potential enhancement of protective immune responses (Figures 1D, E). In contrast, levels of IL-4 and IL-10, which are associated with immunosuppression and exacerbation of cryptococcal diseases, were downregulated following PS-NPs treatment (Figure 1D). Moreover, KEGG pathway analysis revealed an enrichment of immune system-associated terms within the lung tissue of PS-NPs exposed infected mice, particularly highlighting the NF-kappa B signaling pathway (Figure 2A). In the brain of these PS-NPs exposed mice, we observed alterations in immune responses, especially regarding the differentiation of Th1 and Th2 cells (Figure 2B). Overall, PS-NPs

exposure appears to significantly enhance T-cell mediated antifungal immunity in mice infected with *C. neoformans*.

3.2 PS-NPs exposure suppresses *C. neoformans* capsule formation

The capsule of *C. neoformans* induces the expression of *ARG1* to inhibit T-cell mediated antifungal immunity (Li et al., 2022). Our findings demonstrated a decrease in *ARG1* mRNA expression following exposure to PS-NPs (Figure 3A). Subsequently, the size of the *C. neoformans* capsule was examined in mice and capsule induction medium with or without PS-NPs treatment. It was found

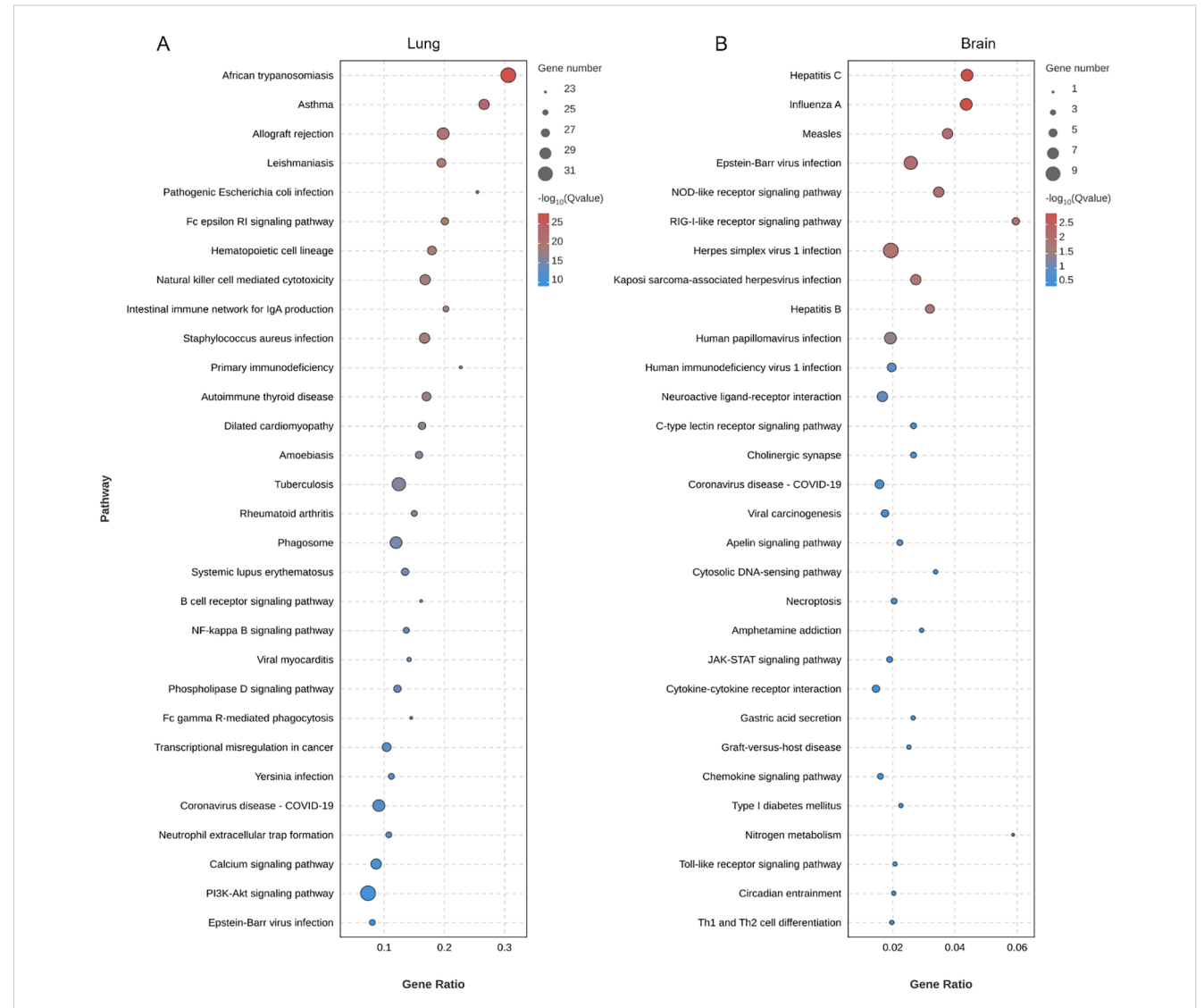
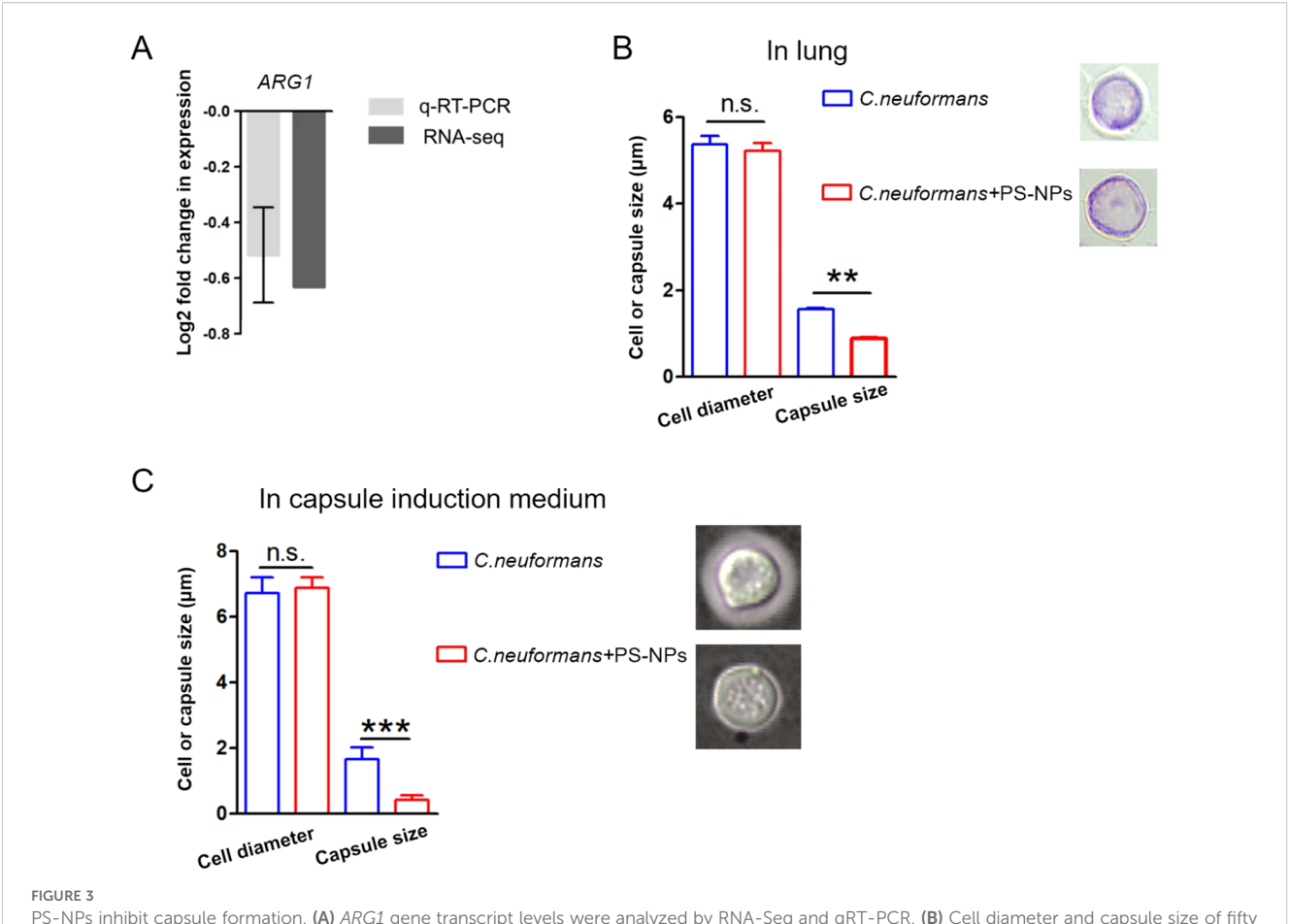


FIGURE 2
Enrichment analysis of KEGG pathways in (A) lung and (B) brain of *C. neoformans*-infected mice treated with PS-NPs. The top 30 enriched KEGG pathways identified through DEGs. Statistical significance for these pathways was assessed using p-values corrected for false discovery rate (FDR), with an FDR threshold set at < 0.05.



PS-NPs inhibit capsule formation. (A) ARG1 gene transcript levels were analyzed by RNA-Seq and qRT-PCR. (B) Cell diameter and capsule size of fifty C. neoformans cells from infected mouse lungs were measured after 28 days of treatment with or without PS-NPs. (C) Cell diameter and capsule size were also measured for fifty C. neoformans cells cultured in capsule induction medium for 18 hours, with or without PS-NPs. Capsule formation was assessed using India ink staining. Statistical analysis via Student's t-test showed significant differences in capsule size, marked by ** (P<0.01) and *** (P<0.001). n.s., not statistically significant.

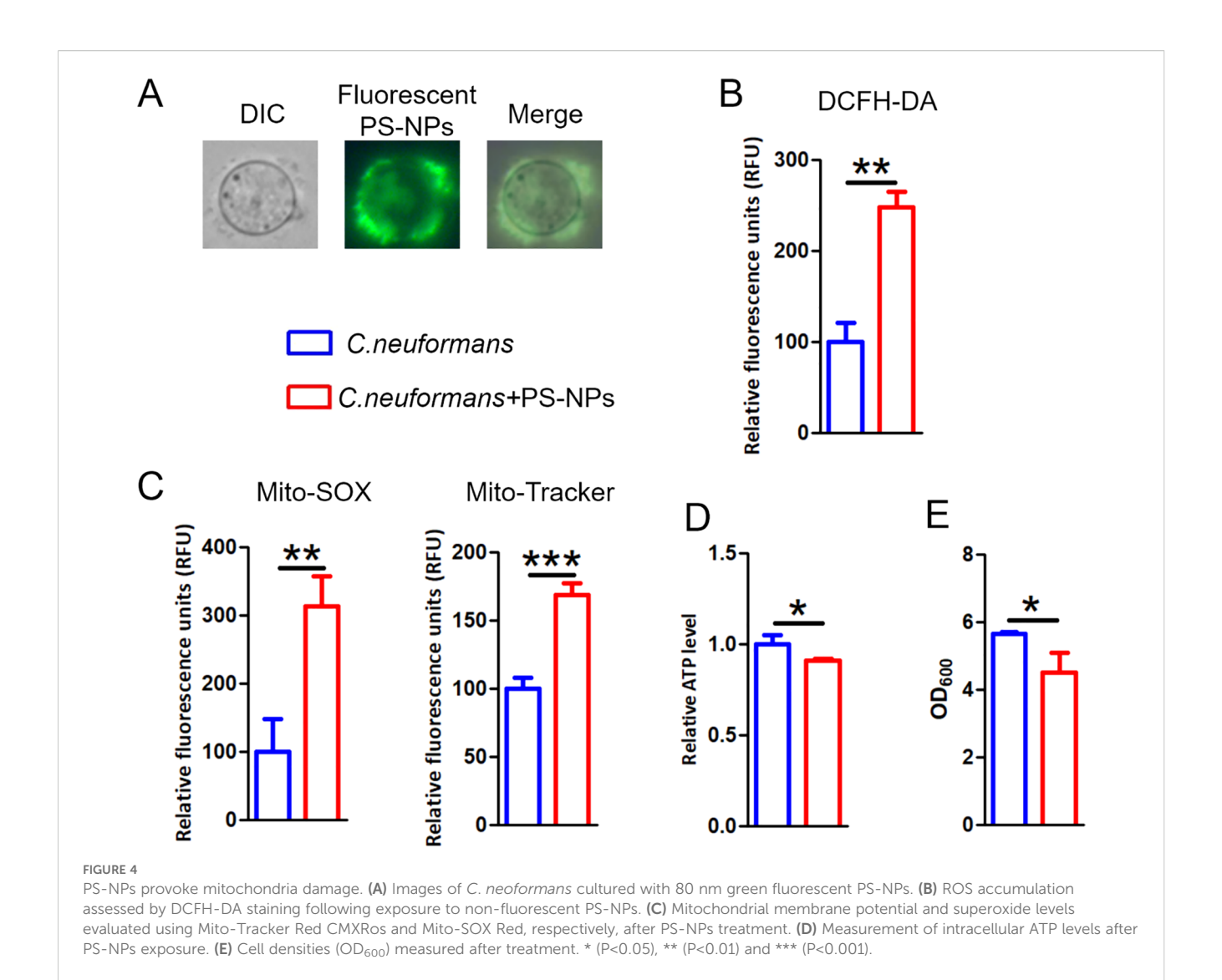
that PS-NPs exposure suppressed the formation of the *C. neoformans* capsule in both mice lungs (Figure 3B) and capsule induction medium (Figure 3C). These results indicate that PS-NPs exposure leads to reduced capsule formation in *C. neoformans*.

3.3 PS-NPs induce *C. neoformans* mitochondrial dysfunction

We first investigated the impact of PS-NPs on ROS levels and mitochondrial function in *C. neoformans*. PS-NPs adhered to the cell wall and entered the cells (Figure 4A). Treatment with PS-NPs led to a significant increase in intracellular ROS levels, as shown by higher DCFH-DA staining compared to untreated cells (Figure 4B). Additionally, we observed that PS-NPs treatment resulted in increased mitochondrial superoxide and membrane potential in *C. neoformans* (Figure 4C). However, this treatment also reduced

intracellular ATP levels (Figure 4D) and inhibited fungal cell growth (Figure 4E).

We further explored the effects of PS-NPs on mitochondrial transcription and metabolism in *C. neoformans*. Our transcriptomic analysis revealed differential expression levels for 474 genes, with 228 genes upregulated and 246 genes downregulated (Figure 5A). GO analysis showed disturbances in molecular function categories related to ATP-dependent and antioxidant activity (Figure 5B). We noted that PS-NPs interfered with mitochondrial transcription, which affected various components, including mitochondrial tricarboxylic acid (TCA) cycle enzyme complexes and the assembly of the mitochondrial respirasome (Figure 5C). Moreover, metabolomics analysis indicated that PS-NPs disrupted mitochondrial metabolic pathways, leading to significant alterations in the TCA cycle and glutathione (GSH) metabolism. Specifically, negative ion MS revealed changes in the TCA cycle (Figure 6A), while positive ion MS showed alterations in GSH metabolism (Figure 6B). Overall, these results



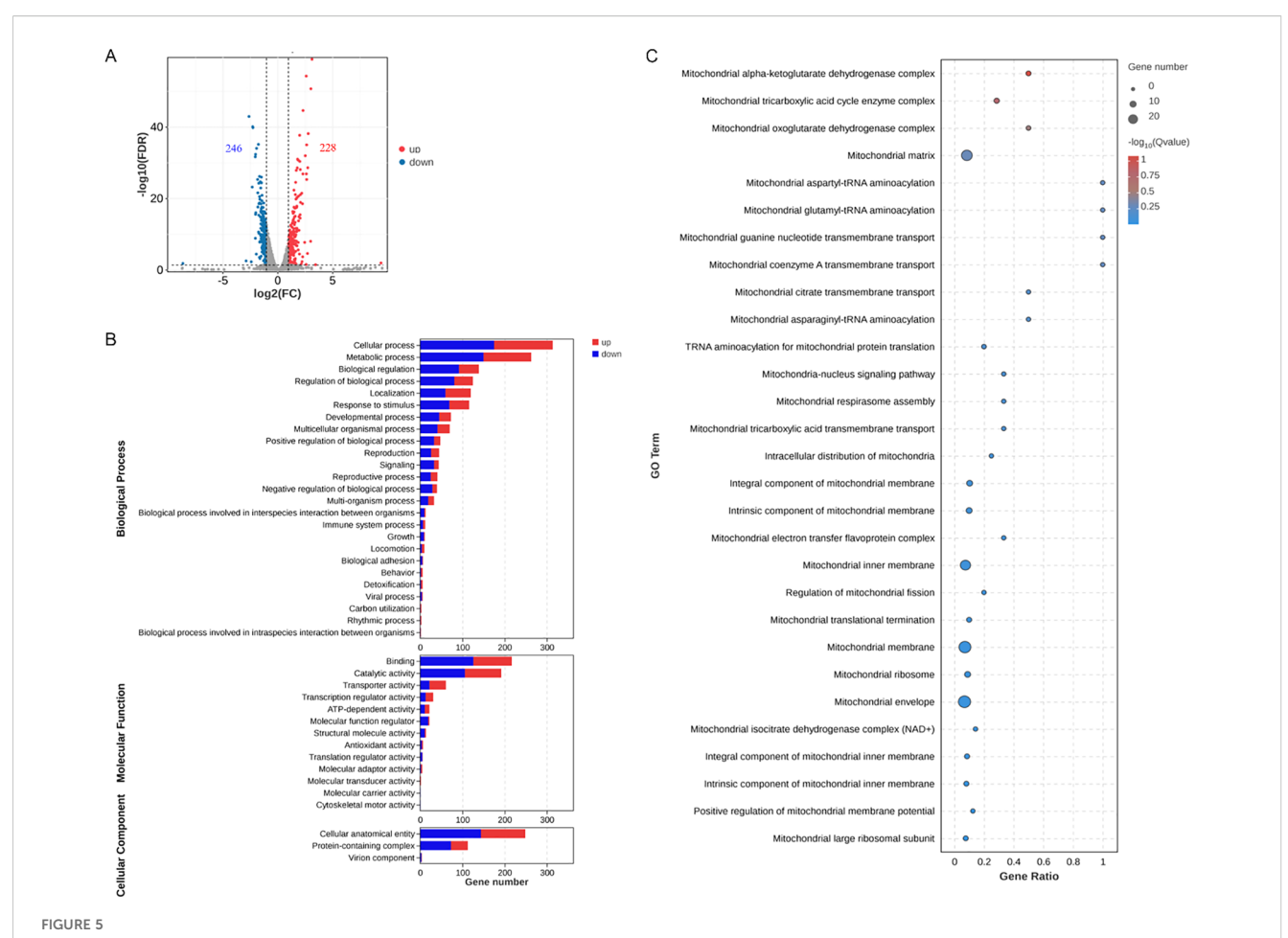
indicate that PS-NPs exposure altered mitochondrial activity, reduced ATP levels, and disrupted TCA and GSH pathways.

4 Discussion

The environmental and toxicological impacts of nanoplastics and microplastics have become significant areas of concern globally, particularly regarding their potential threats to ecosystems and human health (Sana et al., 2020; Mitrano et al., 2021; Aeschlimann et al., 2022; Abdolahpur Monikh et al., 2023; Marfella et al., 2024). A growing body of research indicates that oxidative stress and inflammation are common mechanisms associated with various environmental pollutants (Zheng et al., 2021; Liu et al., 2024), which also apply to exposures from nanoplastics and microplastics. The biological effects of these

pollutants include oxidative stress, inflammatory responses, and genetic toxicity, reflecting their profound impact on living organisms and the environment (Yin et al., 2021; Babaei et al., 2022; Ding et al., 2023; Tang et al., 2023).

This study presents a novel finding: PS-NPs reduce the virulence of *C. neoformans*, potentially via mitochondrial disruption. The dysfunction induced by PS-NPs significantly impacts the metabolic pathways and pathogenicity of *C. neoformans* (Figure 7). Such mitochondrial disruption not only impairs normal physiological processes but may also open new avenues for enhancing antifungal resistance (Ma et al., 2025b). While it is apparent that oxidative damage could drive *C. neoformans* to develop increased resistance to antifungal treatments via genetic mutations or adaptive changes, we must avoid over-speculation in this regard until further data is available. It is important to note that the nanoplastics used in this study were



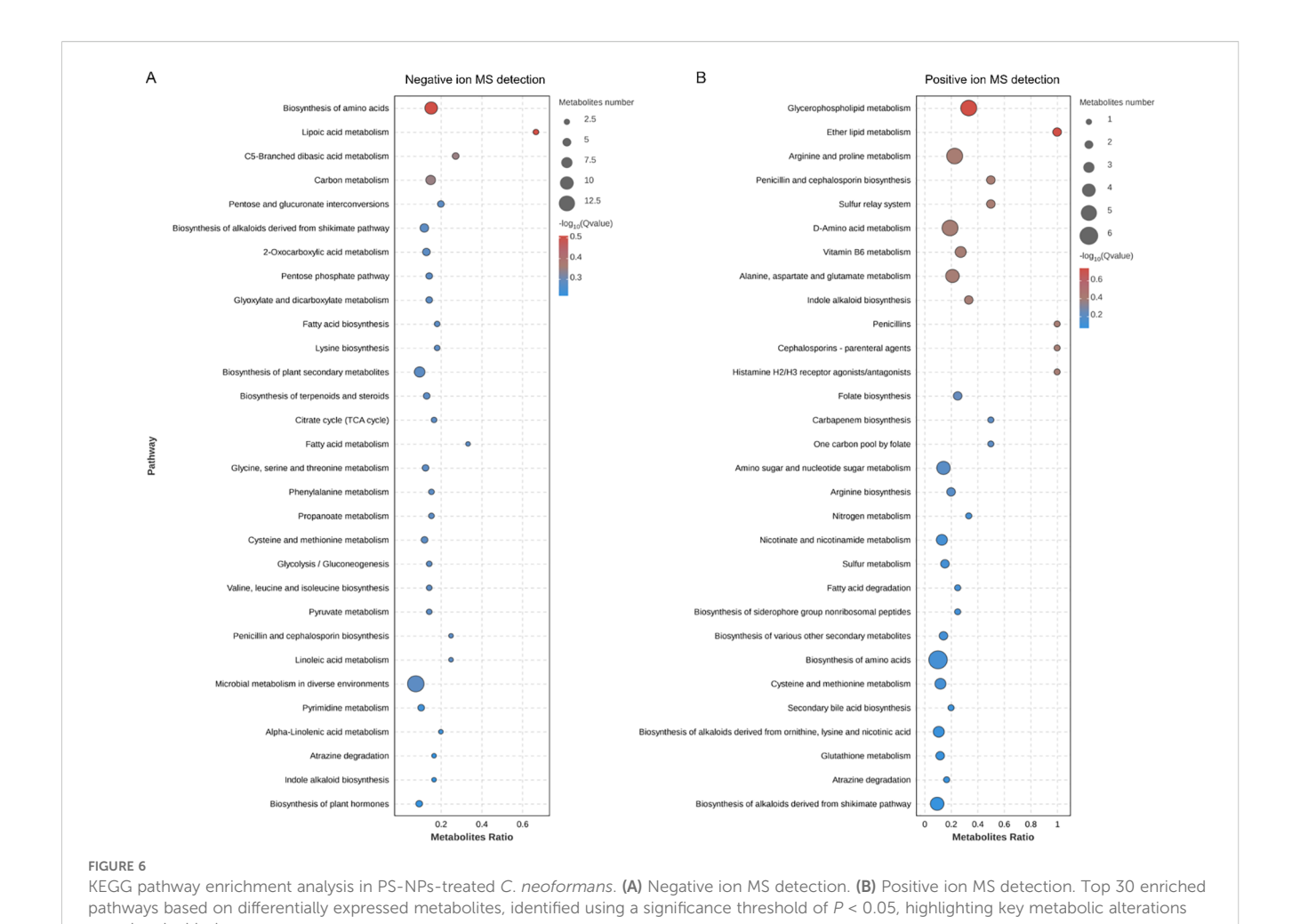
PS-NPs modulate the transcriptional regulation of genes associated with C. neoformans mitochondrial functions. (A) A total of 246 genes were downregulated (green) and 228 genes were upregulated (red) in C. neoformans after treatment with PS-NPs. Differential expression was defined at FDR < 0.05 and fold change \geq 2. (B) GO categories for the differentially expressed genes identified via RNA-seq analysis of C. neoformans cells treated with PS-NPs. (C) Gene Set Enrichment Analysis (GSEA) shows enrichment for the top 30 pathways directly related to mitochondrial function. Improved GO and GSEA pathways highlight disruption of mitochondrial energy and antioxidant functions.

purchased from a commercial supplier, and their shapes may differ from those found in the environment. Additionally, the concentrations of nanoplastics employed in our laboratory setting may vary from those encountered in natural environments. These factors may influence the interactions between nanoplastics and *C. neoformans*, somewhat limiting the generalizability of our findings.

The role of mitochondria in cellular energy metabolism and stress response reinforces their significance in developing potential antifungal therapies. Mitochondria are integral to ATP synthesis and critically influence the activity and expression of drug efflux pumps (Calderone et al., 2015; Black et al., 2021; Xue et al., 2024; Ma et al., 2025a, 2025). Given the emerging focus on mitochondria as targets for novel drugs, understanding the molecular mechanisms behind PS-NP-induced mitochondrial dysfunction could be crucial for devising effective antifungal treatment

strategies. On an ecological scale, the long-term persistence and toxicity of PS-NPs require thorough investigation. Their accumulation in natural environments could disrupt fungal community structures and dynamics, potentially favoring certain species while inhibiting others. Such changes may undermine ecosystem stability and diversity, necessitating future studies to assess the long-term effects of PS-NPs on ecological health.

In summary, the interactions between PS-NPs and *C. neoformans* shed light on the role of nanoplastics in modulating fungal virulence. They also offer insights into environmental factors contributing to fungal resistance, emphasizing the importance of systematic analyses of the environmental and toxicological impacts of PS-NPs. This understanding is paramount for informing public health risk management and guiding future environmental protection strategies.



PS-NPs Mitochondrion disrupted disrupted TCA Cycle GSH metabolism W W W w increased ROS w decreased ATP Inhibition of Capsule formation Th Cryptococcus neoformans Schematic representation of how PS-NPs modulate C. neoformans virulence by inducing mitochondrial dysfunction. PS-NPs induce mitochondrial dysfunction by increasing ROS production and depleting ATP, ultimately inhibiting capsule formation.

associated with the treatment.

Data availability statement

The RNA-Seq data can be accessed in the Genome Sequence Archive (GSA) under the identifiers CRA029802 and CRA029810 at https://ngdc.cncb.ac.cn/gsa. Additionally, the metabolomics data is available in the OMIX database (OMIX011864) at this link: https://ngdc.cncb.ac.cn/omix.

Ethics statement

The animal study was approved by the Experimental Animal Center at Nantong University. The study was conducted in accordance with the local legislation and institutional requirements.

Author contributions

DZ: Writing – review & editing, Visualization, Methodology, Investigation, Writing – original draft, Formal Analysis, Data curation. YZ: Writing – review & editing, Formal Analysis, Writing – original draft, Data curation, Visualization, Methodology, Investigation. BX: Visualization, Formal Analysis, Data curation, Investigation, Writing – review & editing, Writing – original draft. WB: Writing – review & editing, Investigation, Formal Analysis. FW: Writing – review & editing, Investigation, Formal Analysis. XZ: Writing – review & editing, Supervision, Writing – original draft, Formal Analysis, Investigation. PX: Investigation, Supervision, Writing – review & editing, Funding acquisition, Writing – original draft, Formal Analysis, Project administration. YM: Project administration, Formal Analysis, Supervision, Writing – original draft, Funding acquisition, Writing – review & editing, Investigation.

Funding

The author(s) declare financial support was received for the research and/or publication of this article. This research was supported by the Natural Science Research of Jiangsu Higher Education Institutions of China (No. 24KJD430010), the Nantong

Jiangsu Scientific Research Project of China (No. JC2023043), the Natural Science Foundation of Jiangsu Province of China (No. BK20240948), and the Postgraduate Research & Practice Innovation Program of Jiangsu Province (KYCX24_3537, KYCX24_3538).

Conflict of interest

The authors declare that the research was conducted in the absence of any commercial or financial relationships that could be construed as a potential conflict of interest.

Generative AI statement

The author(s) declare that no Generative AI was used in the creation of this manuscript.

Any alternative text (alt text) provided alongside figures in this article has been generated by Frontiers with the support of artificial intelligence and reasonable efforts have been made to ensure accuracy, including review by the authors wherever possible. If you identify any issues, please contact us.

Publisher's note

All claims expressed in this article are solely those of the authors and do not necessarily represent those of their affiliated organizations, or those of the publisher, the editors and the reviewers. Any product that may be evaluated in this article, or claim that may be made by its manufacturer, is not guaranteed or endorsed by the publisher.

Supplementary material

The Supplementary Material for this article can be found online at: https://www.frontiersin.org/articles/10.3389/fcimb.2025. 1708192/full#supplementary-material

SUPPLEMENTARY TABLE 1

Primer sequences used for qRT-PCR. F: forward primer; R: reverse primer.

References

Abdolahpur Monikh, F., Baun, A., Hartmann, N. B., Kortet, R., Akkanen, J., Lee, J. S., et al. (2023). Exposure protocol for ecotoxicity testing of microplastics and nanoplastics. *Nat. Protoc.* 18, 3534–3564. doi: 10.1038/s41596-023-00886-9

Aeschlimann, M., Li, G., Kanji, Z. A., and Mitrano, D. M. (2022). Potential impacts of atmospheric microplastics and nanoplastics on cloud formation processes. *Nat. Geosci.* 15, 967–975. doi: 10.1038/s41561-022-01051-9

Ashburner, M., Ball, C. A., Blake, J. A., Botstein, D., Butler, H., Cherry, J. M., et al. (2000). Gene ontology: tool for the unification of biology. *Nat. Genet.* 25, 25–29. doi: 10.1038/75556

Babaei, A. A., Rafiee, M., Khodagholi, F., Ahmadpour, E., and Amereh, F. (2022). Nanoplastics-induced oxidative stress, antioxidant defense, and physiological response in exposed Wistar albino rats. *Environ. Sci pollut. Res.* 29 (8), 11332–11344. doi: 10.1007/s11356-021-15920-0

Barguilla, I., Domenech, J., Ballesteros, S., Rubio, L., Marcos, R., and Hernández, A. (2022). Long-term exposure to nanoplastics alters molecular and functional traits related to the carcinogenic process. *J. Hazardous Materials* 438, 129470. doi: 10.1016/ijhazmat.2022.129470

Black, B., Lee, C., Horianopoulos, L. C., Jung, W. H., and Kronstad, J. W. (2021). Respiring to infect: Emerging links between mitochondria, the electron transport chain, and fungal pathogenesis. *PloS Pathog.* 17, e1009661. doi: 10.1371/journal.ppat.1009661

Bu, W., Yu, M., Ma, X., Shen, Z., Ruan, J., Qu, Y., et al. (2025). Gender-specific effects of prenatal polystyrene nanoparticle exposure on offspring lung development. *Toxicol. Lett.* 407, 1–16. doi: 10.1016/j.toxlet.2025.03.001

Calderone, R., Li, D., and Traven, A. (2015). System-level impact of mitochondria on fungal virulence: to metabolism and beyond. *FEMS yeast Res.* 15, fov027. doi: 10.1093/femsyr/fov027

Casalini, G., Giacomelli, A., and Antinori, S. (2024). The WHO fungal priority pathogens list: a crucial reappraisal to review the prioritisation. *Lancet Microbe* 5, 717–724. doi: 10.1016/S2666-5247(24)00042-9

- Cheng, D., Zheng, D., Jiang, M., Jin, Y., Liu, R., Zhou, Y., et al. (2025). Inhibition of iron ion accumulation alleviates polystyrene nanoplastics-induced pulmonary fibroblast proliferation and activation. *Int. Immunopharmacol* 164, 115367. doi: 10.1016/j.intimp.2025.115367
- Ding, R., Ma, Y., Li, T., Sun, M., Sun, Z., and Duan, J. (2023). The detrimental effects of micro-and nano-plastics on digestive system: An overview of oxidative stress-related adverse outcome pathway. *Sci Total Environ.* 878, 163144. doi: 10.1016/j.scitotenv.2023.163144
- Ding, Y., Zhang, R., Li, B., Du, Y., Li, J., Tong, X., et al. (2021). Tissue distribution of polystyrene nanoplastics in mice and their entry, transport, and cytotoxicity to GES-1 cells. *Environ. pollut.* 280, 116974. doi: 10.1016/j.envpol.2021.116974
- Dunn, W. B., Broadhurst, D., Begley, P., Zelena, E., Francis-McIntyre, S., Anderson, N., et al. (2011). Procedures for large-scale metabolic profiling of serum and plasma using gas chromatography and liquid chromatography coupled to mass spectrometry. *Nat. Protoc.* 6, 1060–1083. doi: 10.1038/nprot.2011.335
- Huffnagle, G. B., Yates, J., and Lipscomb, M. F. (1991). Immunity to a pulmonary Cryptococcus neoformans infection requires both CD4+ and CD8+ T cells. *J. Exp. Med.* 173, 793–800. doi: 10.1084/jem.173.4.793
- Jung, W. H., Sham, A., Lian, T., Singh, A., Kosman, D. J., and Kronstad, J. W. (2008). Iron source preference and regulation of iron uptake in Cryptococcus neoformans. *PloS Pathog.* 4, e45. doi: 10.1371/journal.ppat.0040045
- Kanehisa, M., and Goto, S. (2000). KEGG: kyoto encyclopedia of genes and genomes. Nucleic Acids Res. 28, 27–30. doi: 10.1093/nar/28.1.27
- Li, Y. N., Wang, Z. W., Li, F., Zhou, L. H., Jiang, Y. S., Yu, Y., et al. (2022). Inhibition of myeloid-derived suppressor cell arginase-1 production enhances T-cell-based immunotherapy against *Cryptococcus neoformans* infection. *Nat. Commun.* 13, 4074. doi: 10.1038/s41467-022-31723-4
- Li, Z., Xu, T., Peng, L., Tang, X., Chi, Q., Li, M., et al. (2023). Polystyrene nanoplastics aggravates lipopolysaccharide-induced apoptosis in mouse kidney cells by regulating IRE1/XBP1 endoplasmic reticulum stress pathway via oxidative stress. J. Cell. Physiol. 238, 151-164. doi: 10.1002/jcp.30913
- Liu, L., Luo, C., Zheng, D., Wang, X., Wang, R., Ding, W., et al. (2024). TRPML1 contributes to antimony-induced nephrotoxicity by initiating ferroptosis *via* chaperone-mediated autophagy. *Food Chem. Toxicol.* 184, 114378. doi: 10.1016/j.fct.2023.114378
- Liu, X., Zhao, Y., Dou, J., Hou, Q., Cheng, J., and Jiang, X. (2022). Bioeffects of inhaled nanoplastics on neurons and alteration of animal behaviors through deposition in the brain. *Nano Lett.* 22, 1091–1099. doi: 10.1021/acs.nanolett.1c04184
- Ma, Y., Zhou, Y., Jia, T., Zhuang, Z., Xue, P., and Yang, L. (2025a). Deciphering the role of mitochondria in human fungal drug resistance. *Mycology*, 1–14. doi: 10.1080/21501203.2025.2473507

- Ma, Y., Zhou, Y., Zheng, D., Bu, W., Wang, F., Zhao, X., et al. (2025b). Nanoplastics and fungi: exploring dual roles in degradation and pathogenicity. *Front. Microbiol. Volume* 16. doi: 10.3389/fmicb.2025.1679160
- Marfella, R., Prattichizzo, F., Sardu, C., Fulgenzi, G., Graciotti, L., Spadoni, T., et al. (2024). Microplastics and nanoplastics in atheromas and cardiovascular events. *New Engl. J. Med.* 390, 900–910. doi: 10.1056/NEJMoa2309822
- Mitrano, D. M., Wick, P., and Nowack, B. (2021). Placing nanoplastics in the context of global plastic pollution. *Nat. Nanotechnology* 16, 491–500. doi: 10.1038/s41565-021-00888-2
- Park, B. J., Wannemuehler, K. A., Marston, B. J., Govender, N., Pappas, P. G., and Chiller, T. M. (2009). Estimation of the current global burden of cryptococcal meningitis among persons living with HIV/AIDS. *Aids* 23, 525–530. doi: 10.1097/QAD.0b013e328322ffac
- Rajasingham, R., Smith, R. M., Park, B. J., Jarvis, J. N., Govender, N. P., Chiller, T. M., et al. (2017). Global burden of disease of HIV-associated cryptococcal meningitis: an updated analysis. *Lancet Infect. Dis.* 17, 873–881. doi: 10.1016/S1473-3099(17)30243-8
- Saikia, S., Oliveira, D., Hu, G., and Kronstad, J. (2014). Role of ferric reductases in iron acquisition and virulence in the fungal pathogen *Cryptococcus neoformans*. *Infection Immun.* 82, 839–850. doi: 10.1128/IAI.01357-13
- Sana, S. S., Dogiparthi, L. K., Gangadhar, L., Chakravorty, A., and Abhishek, N. (2020). Effects of microplastics and nanoplastics on marine environment and human health. *Environ. Sci pollut. Res.* 27, 44743–44756. doi: 10.1007/s11356-020-10573-x
- Tang, J., Bu, W., Hu, W., Zhao, Z., Liu, L., Luo, C., et al. (2023). Ferroptosis is involved in sex-specific small intestinal toxicity in the offspring of adult mice exposed to polystyrene nanoplastics during pregnancy. *ACS nano* 17, 2440–2449. doi: 10.1021/acsnano.2c09729
- Vartivarian, S. E., Anaissie, E. J., Cowart, R. E., Sprigg, H. A., Tingler, M. J., and Jacobson, E. S. (1993). Regulation of cryptococcal capsular polysaccharide by iron. *J. Infect. Dis.* 167, 186–190. doi: 10.1093/infdis/167.1.186
- Warnes, G. R., Bolker, B., Lumley, T., and Johnson, R. C. (2015). gmodels: Various R programming tools for model fitting. *R package version 2.16.2*. Available online at: https://CRAN.R-project.org/package=gmodels.
- Xue, P., Sánchez-León, E., Hu, G., Lee, C. W., Black, B., Brisland, A., et al. (2024). The interplay between electron transport chain function and iron regulatory factors influences melanin formation in *Cryptococcus neoformans*. *Msphere* 9 (5), e00250–e00224. doi: 10.1128/msphere.00250-24
- Yin, K., Wang, Y., Zhao, H., Wang, D., Guo, M., Mu, M., et al. (2021). A comparative review of microplastics and nanoplastics: Toxicity hazards on digestive, reproductive and nervous system. *Sci total Environ.* 774, 145758. doi: 10.1016/j.scitotenv.2021.145758
- Zhai, Y., Guo, W., Li, D., Chen, B., Xu, X., Cao, X., et al. (2024). Size-dependent influences of nanoplastics on microbial consortium differentially inhibiting 2, 4-dichlorophenol biodegradation. *Water Res.* 249, 121004. doi: 10.1016/j.watres.2023.121004
- Zheng, Y., Ding, W., Zhang, T., Zhao, Z., Wang, R., Li, Z., et al. (2021). Antimony-induced astrocyte activation *via* mitogen-activated protein kinase activation-dependent CREB phosphorylation. *Toxicol. Lett.* 352, 9–16. doi: 10.1016/j.toxlet.2021.09.006